Journal of Applied Toxicology

WILEY

Journal of AppliedToxicology

RESEARCH ARTICLE OPEN ACCESS

Epirubicin Alters Pancreatic Autophagy and Insulin Synthesis Through a Zinc-Dependent Mechanism

Ebru Afşar[1] | Işıl Eranıl[2]

[1]Department of Biochemistry, Faculty of Dentistry, Cappadocia University, Nevşehir, Turkey | [2]Department of Medical Services and Techniques, Cappadocia Vocational School, Cappadocia University, Nevşehir, Turkey

Correspondence: Ebru Afşar (ebru.afsar@kapadokya.edu.tr; ebrukiracc@gmail.com)

Received: 18 February 2026 | **Revised:** 15 May 2026 | **Accepted:** 27 May 2026

Keywords: chemotherapy-induced diabetes | epirubicin | zinc transporters

ABSTRACT

Epirubicin (EPI) can cause metabolic side effects, including chemotherapy-related diabetes, partly through oxidative stress that disrupts zinc (Zn) homeostasis and impairs autophagy. This study investigated the effects of EPI on Zn regulation and autophagy in the pancreas, as well as the modulatory role of *N*-acetylcysteine (NAC). Rats received EPI (9.6 mg/kg) by intraperitoneal injection (i.p.) followed 1 h later by NAC (50 or 300 mg/kg, i.p.). Glucose homeostasis was assessed using the Homeostatic Model Assessment (HOMA-IR), and β-cell function was assessed using HOMA-β levels. Plasma insulin levels, as well as insulin, proinsulin, beclin, autophagy-related proteins (ATG5), Microtubule-Associated Protein 1 Light Chain 3 (LC3), phosphorylated Akt (p-Akt), mechanistic target of rapamycin complex 1 (mTOR1), cleaved caspase-3, Zrt/Irt-like Protein 10 (ZIP10), and the proliferation marker Ki-67 in pancreatic tissue, were measured using commercial ELISA kits. Total oxidant status (TOS) and total antioxidant status (TAS) were measured using commercial colorimetric assay kits, and the oxidative stress index (OSI) was calculated. Zn levels in pancreatic tissue and plasma samples were measured using a colorimetric method. Morphological changes in the pancreas were assessed by hematoxylin and eosin staining. As a result, in the EPI group, oxidative stress and ZIP10 levels increased, whereas Zn levels decreased, as well as pancreatic autophagy, proliferation, and insulin synthesis increased. Oxidative stress decreased in both the EN-50 and EN-300 groups, with a more pronounced decrease in the EN-300 group. Furthermore, in the EN-300 group, pancreatic Zn, ZIP10, autophagy, and proliferation levels decreased, whereas mTOR1 levels increased. The pancreatic insulin synthesis observed in the EN-50 group was not observed in the EN-300 group. In conclusion, the increased autophagy observed in the Epi group may reflect an adaptive response to oxidative stress. The effects of NAC on oxidative stress may be dose-dependent, and high-dose NAC administration may suppress EPI-induced autophagy via mTOR1-mediated signaling. Furthermore, the relationship among Zn levels, autophagy, and insulin synthesis observed in the experimental groups may contribute to a better understanding of EPI-associated diabetogenic alterations.

1 | Introduction

Epirubicin (EPI) is a chemotherapeutic agent used in various malignancies; however, its clinical application is significantly restricted by severe adverse effects (Petit et al. 2020). EPI exerts its anticancer effects by inhibiting cancer proliferation, inhibiting topoisomerase, and generating reactive oxygen species (ROS), which are also responsible for its side effects. These processes damage vital biomolecules and cause cell death (Alves et al. 2016), which can damage pancreatic islets and accelerate the development of diabetes mellitus (DM). A 2016 case report described an individual with breast cancer treated with EPI

who developed symptoms suggestive of DM after chemotherapy (Sharma et al. 2016). However, the exact molecular changes that EPI causes in pancreatic cells are not known.

Autophagy plays an essential role in cell differentiation and survival, and is necessary to maintain homeostasis under physiological conditions (Kong et al. 2017). It recycles cellular components through autophagic flux, which encompasses autophagosome formation, lysosomal fusion, degradation, and macromolecule release (Tuohetaerbaike et al. 2020). Various growth and nutrient signals regulate autophagy in response to stress. Growth factors activate the phosphatidylinositol-3-kinase (PI3K)/protein kinase B (Akt)/(mechanistic target of rapamycin complex) 1 (mTORC1), which suppresses autophagy. When ATP levels decrease, activation of adenosine 5′-monophosphate (AMP)-activated protein kinase (AMPK) inhibits mTORC1 and activates the autophagy machinery (Pasquier 2016; Tuohetaerbaike et al. 2020).

Autophagy is also essential for pancreatic cell survival (Kong et al. 2017) and insulin secretion (Sheng et al. 2017). Regulating autophagy is critical for maintaining β-cell survival and pancreatic function. Many studies have demonstrated that zinc (Zn) is vital for β-cell function, including insulin processing and secretion (Gyulkhandanyan et al. 2008), and that it promotes autophagy (Liuzzi and Pazos 2020). Furthermore, evidence suggests that Zrt/Irt-like Protein 10 (ZIP10) facilitates the transport of extracellular Zn into cells, thereby increasing cellular Zn levels (Jeong and Eide 2013), and conferring chemoprotective properties (Li et al. 2021). This information suggests that ZIP10-mediated Zn regulation in EPI-induced diabetic symptoms may play a role in pancreatic autophagy and function, and that modulation of oxidative stress index (OSI), which is responsible for EPI side effects, may be beneficial in influencing these changes. Therefore, understanding the biological effects of Zn may help clarify the mechanisms underlying pancreatic responses to oxidative stress and chemotherapeutic injury.

N-acetylcysteine (NAC) is a multi-target drug and dietary supplement with antioxidant and anti-inflammatory effects. NAC also supports glutathione synthesis (GSH), thereby preventing oxidative stress and cell damage (11), which in turn affects β-cells and insulin target cells (12). Therefore, we investigated how EPI affects ZIP10-mediated changes in pancreatic Zn levels, the impact of these changes on autophagy and glucose homeostasis, and whether NAC has a beneficial effect.

2 | Materials and Methods

2.1 | Animals and Experimental Design

Male albino Wistar rats (aged 3 months) from Aksaray University were used following institutional ethical approval (2025/4–37). All rats were housed in controlled conditions (temperature 23°C ± 1°C, humidity 50% ± 5%, and a 12-h light/dark cycle), and had ad libitum access to standard chow and water.

Figure 1 shows the experimental design, including the animal model and the measured parameters. Animals were randomly assigned to four experimental groups ($n = 6$ per group).

Control group: Rats received i.p. saline followed by a second i.p. saline injection 1 h later. This group served as both the untreated and the vehicle control.

EPI-treated group (Epi group): Rats received i.p. saline, followed 1 h later by EPI (9.6 mg/kg, i.p.). This group was used to evaluate the effects of EPI alone.

NAC-treated group (Nac group): Rats received NAC (300 mg/kg, i.p.) followed 1 h later by a second i.p. saline injection (equivalent volume to EPI). This group was included to evaluate the independent effects of NAC while maintaining the same injection frequency and experimental conditions as the EPI-treated groups.

Combination groups: Rats received NAC prior to EPI administration to evaluate its potential protective effects. Specifically, one group received low-dose NAC (50 mg/kg, i.p.) 1 h before EPI injection (EN-50 group), and another group received high-dose NAC (300 mg/kg, i.p.) 1 h before EPI injection (EN-300 group).

Five days post-treatment, animals were anesthetized and sacrificed. EPI (Dobbs et al. 2003; Dobbs et al. 1994; Devaleriola 1994) and NAC doses were based on previous literature (Sabbaghziarani et al. 2024; Kalimeris et al. 2016), and all compounds were obtained from Sigma-Aldrich (St. Louis, MO, USA).

2.1.1 | Determination of Experimental EPI Dose

The typical EPI dose administered to patients undergoing chemotherapy is 60 mg/m^2, equivalent to approximately 1.56 mg/kg in humans. The rat-equivalent dose was calculated using body surface area normalization with Km factors (human Km = 37; rat Km = 6) according to the following formula: Human equivalent dose (HED, mg/kg) = Animal dose (mg/kg) × (Animal Km/Human Km). Accordingly, the rat-equivalent dose was 9.6 mg/kg. Therefore, a 9.6 mg/kg EPI dose was used in rats, corresponding to the commonly administered human chemotherapy dose of 60 mg/m^2 (Nair and Jacob 2016).

2.1.2 | Determination of Experimental NAC Dose

Previous studies have reported that NAC administration at 50 mg/kg (Sabbaghziarani et al. 2024) is beneficial. Therefore, in this study, lower (50 mg/kg) and higher (300 mg/kg) NAC doses will be used to evaluate the efficacy of low and high NAC doses in EPI rats (Kalimeris et al. 2016). This approach was intended to capture a broader therapeutic range.

2.2 | Biochemical Analysis

Tissue samples were homogenized in phosphate-buffered saline (PBS) at a 1:9 (w/v) ratio. The homogenates were centrifuged at 10,000 × *g* for 5 min at 4°C, and the supernatants were collected for biochemical analyses. Plasma samples were obtained by centrifuging whole blood at 1500 × g for 15 min. All samples were stored at −80°C for biochemical analysis (Afsar

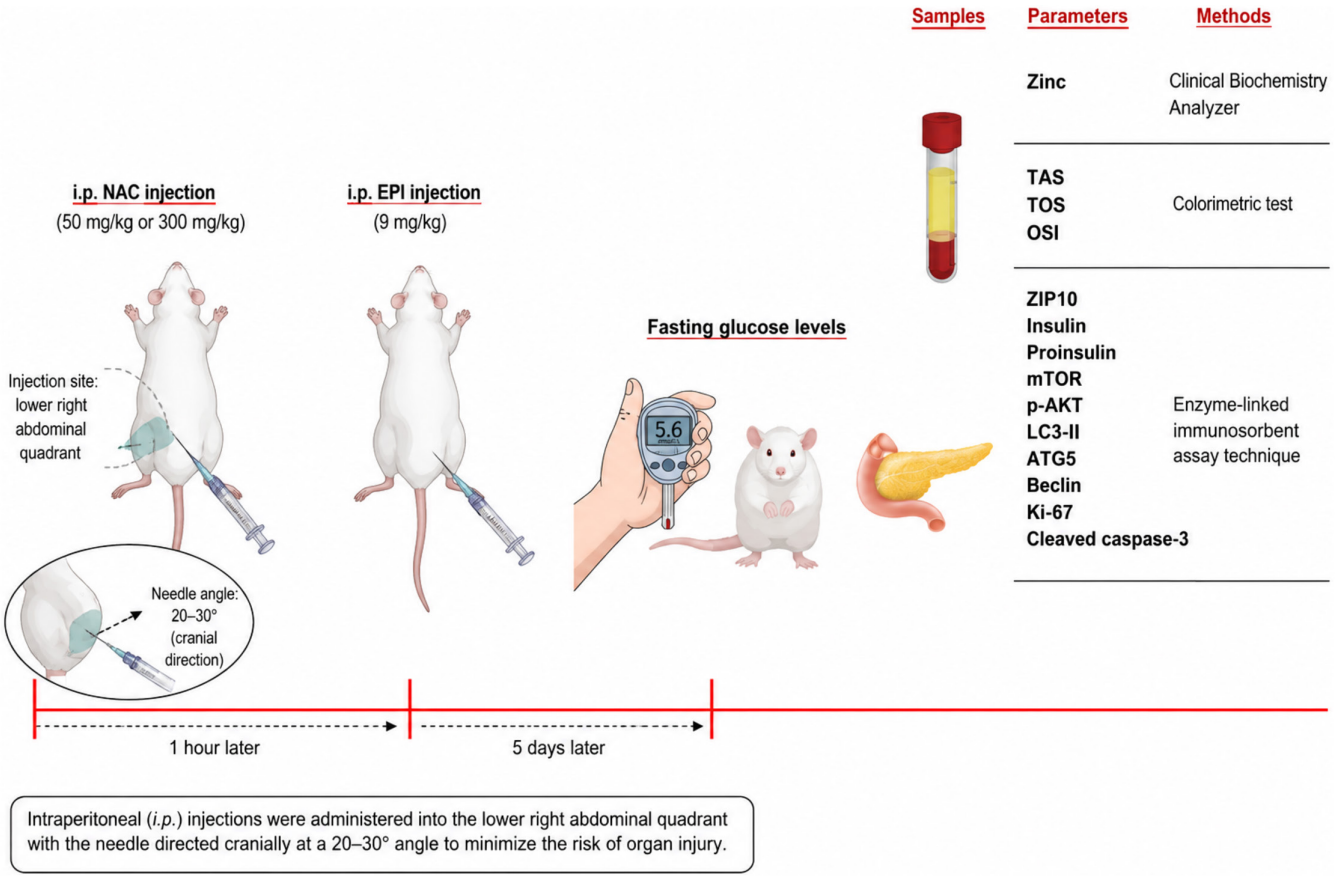

FIGURE 1 | Experimental design. Epirubicin (9.6 mg/kg) was injected by i.p. injection, and 1 h later, the NAC (50 mg/kg or 300 mg/kg) was injected by i.p. injection. Fasting glucose levels were measured using a glucometer; a biochemistry analyzer was used for zinc levels of plasma and pancreas tissue, and an ELISA assay was used for other parameters. Abbreviations: EPI, Epirubicin; i.p., intraperitoneal; mTOR, mammalian target of rapamycin; NAC, N-acetylcysteine; OSI, oxidative stress index; p-AKT, phosphorylated Protein kinase B; TAS, total antioxidant status; TOS, total oxidant status.

and Kantar 2025). Plasma insulin levels and pancreatic tissue levels of insulin, proinsulin, beclin, autophagy-related proteins (ATG5), Microtubule-Associated Protein 1 Light Chain 3 (LC3), phosphorylated Akt (p-Akt), mTOR1, cleaved caspase-3, ZIP10, and Ki-67 were measured using commercial ELISA kits (Bioassay Technology Laboratory, BT Lab). The method is based on antigen–antibody binding and HRP-mediated color development, and absorbance was measured spectrophotometrically at 450 nm (Afsar, Öz, and Eranil 2026). Zn concentrations in plasma and pancreatic tissue were determined by a colorimetric assay on a fully automated clinical biochemistry analyzer (Mindray BS400).

2.2.1 | Fasting Glucose Measurement

Animals were fasted overnight before testing, and glucose levels were determined using a glucometer (Accuro, pM1–300, Bionime Corporation, Taiwan) by blood collected from the tail (Afsar, Dogan, et al. 2026).

2.2.2 | Homeostatic Model Assessment (HOMA)

Insulin resistance (HOMA-IR) was calculated as fasting insulin (mIU/L) × fastingglucose(mM) ÷ 22.5. β-Cellfunction(HOMA-β) was estimated using the formula: (HOMA-β) % = [360 × fasting insulin (μIU/ml)] / (fasting glucose (mg/dl) − 63) (Abdulmalek and Balbaa 2019).

2.2.3 | Total Oxidant and Antioxidant Status

Total oxidant status (TOS) and total antioxidant status (TAS) measurement: TOS and TAS levels were measured using a colorimetric assay (Rel Assay Diagnostic). The principle of TOS analysis is based on the oxidation of the ferrous ion–*o*-dianisidine complex to ferric ions by oxidant molecules present in the sample. The ferric ions subsequently form a colored complex with xylenol orange under acidic conditions. The color intensity, measured at 530 nm spectrophotometrically, is directly proportional to the total number of oxidant molecules in the sample. The principle of TAS analysis is based on the reduction of the characteristic color of the ABTS (2,2′-azino-bis[3-ethylb enzothiazoline-6-sulfonic acid]) radical cation by antioxidants present in the sample. The decrease in color intensity was measured colorimetrically at 660 nm and reflects the sample's total antioxidant capacity.

The oxidative stress index (OSI) was calculated as OSI (arbitrary units) = TOS (μmol H_2O_2 equivalent/L)/TAS (μmol Trolox equivalent/L) (Ozturk et al. 2011).

All tissue sample results were normalized to tissue protein content, as described in an earlier study (Afsar and Kantar 2025; Afsar, Dogan, et al. 2026). Protein concentrations were determined at 595 nm using a modified Bradford assay with Coomassie Plus reagent, using bovine serum albumin as the standard (Pierce Chemical Company, Rockford, Illinois, USA) (Bradford 1976).

2.3 | Histopathologic Examinations of Pancreatic Tissues

Pancreatic tissues were fixed in 10% paraformaldehyde, embedded in paraffin, and sectioned at 5–6 μm thickness. The sections were stained with hematoxylin and eosin (H&E) and examined under a light microscope (Leica DFC450, Germany). Histopathological alterations, including cellular degeneration, cytoplasmic vacuolization, and contour irregularities, were evaluated semi-quantitatively in a blinded manner. Tissue injury was scored according to the severity of histopathological changes as follows: 0 = no lesion; 1 = mild; 2 = moderate; and 3 = severe. Total histopathological scores were calculated from the examination of multiple randomly selected fields at identical magnification (Periyanayagam et al. 2015; Dur et al. 2016; Afsar, Dogan, et al. 2026).

2.4 | Statistical Analysis

All statistical analyses were conducted in SPSS 23.0 (SPSS, Chicago, Illinois, USA) for Windows. For normally distributed data, one-way ANOVA was followed by Tukey's post hoc test. For non-normally distributed data, the Kruskal–Wallis test was followed by Mann–Whitney U tests, and multiple comparisons were corrected using the Benjamini–Hochberg false discovery rate (FDR) procedure (Lee and Lee 2020). All values are presented as mean ± SD, $n = 6$ per group, and $q < 0.05$ was considered significant. The importance of appropriately determining sample size in scientific studies has been highlighted previously. Sample size estimation was performed using power analysis based on effect-size calculations (Shojaee Barjoee et al. 2025). Power analysis was performed using G*Power (version 3.1.9.7). The calculation was based on five independent groups, an $\alpha = 0.05$ significance level, and a desired statistical power of 0.80 (Ersoz et al. 2023). Accordingly, $n = 6$ in each group. Histological data were analyzed with the Kruskal-Wallis test followed by Dwass–Steel–Critchlow–Fligner post hoc test.

3 | Results

3.1 | Analysis of Glucose Homeostasis and Insulin Synthesis

Pairwise comparisons indicated that HOMA-IR levels were significantly lower in the EN-300 group than in the EN-50 group ($p < 0.05$). In addition, plasma insulin levels were lower in the EN-300 group than in the EN-50 group ($p < 0.05$). Pancreatic insulin levels were significantly higher in the Epi group than in the control group ($p < 0.05$), and higher in the EN-50 group than in the EPI group ($p < 0.05$) and the EN-300 group ($p < 0.05$).

HOMA-β levels were significantly higher in the Epi group than in the control group ($p < 0.05$). No significant difference was observed between the groups in fasting blood glucose levels. Results are shown in Table 1.

3.2 | Analysis of Autophagy and Proliferation-Related Parameters

The results of the analysis of autophagy- and proliferation-related parameters are presented in Table 2.

LC3 levels in the control group were significantly lower than in the NAC group ($p < 0.05$) and the Epi group ($p < 0.05$), and in the EN-300 group were significantly lower than in the EN-50 group ($p < 0.05$).

ATG-5 levels in the control group were significantly lower than in the EPI group ($p < 0.01$). NAC administration decreased ATG-5 levels in the EN-300 group compared with the EN-50 group ($p < 0.01$). No difference in ATG5 levels was observed between the control and NAC groups ($p > 0.05$).

Pancreatic beclin levels in the EN-50 group were significantly higher than in the EPI group ($p < 0.05$) and in the EN-300 group

TABLE 1 | Evaluation of changes of glucose homeostasis and insulin synthesis between groups.

	Control	NAC	EPI	EN-50	EN-300
Fasting blood glucose levels (mg/dL)	105 ± 2.966	99 ± 3.98	105 ± 10.068	98 ± 6.802	107 ± 5.820
Plasma insulin levels (mIU/L)	0.556 ± 0.424	0.601 ± 0.258	0.787 ± 0.302	1.079 ± 0.267	0.606 ± 0.204[b]
HOMA-IR levels	2.648 ± 2.001	2.734 ± 1.219	3.619 ± 1.169	4.859 ± 1.056	2.941 ± 1.053[b]
HOMA-β levels (%)	4.136 ± 3.420	6.389 ± 2.546	7.231 ± 4.415*	10.019 ± 4.480	5.463 ± 1.486
Pancreas pro-insulin levels (ng/g protein)	3.484 ± 1.494	5.517 ± 1.526	5.957 ± 2.115	6.373 ± 2.060*	3.750 ± 1.031
Pancreas insulin levels (mIU/g protein)	0.355 ± 0.147	0.601 ± 0.258	0.633 ± 0.157*	1.079 ± 0.267[a]	0.606 ± 0.204[b]

Note: Statistical analysis was performed using Kruskal–Wallis's One-Way Analysis of Variance on Ranks. Pairwise comparisons were performed using the Mann–Whitney U test, and *p*-values were adjusted for multiple comparisons using the Benjamini–Hochberg false discovery rate procedure. All values are mean ± SD, $n = 6$ for each group.
*$p < 0.05$ vs. control.
[a]$p < 0.001$ vs. EPI.
[b]$p < 0.05$ vs. EN-50.

($p < 0.01$). No difference in beclin levels was observed between the control and NAC groups or between the control and EPI groups ($p > 0.05$).

p-Akt levels in the control group were lower than in the NAC group ($p < 0.05$), and in the EN-300 group were lower than in the EN-50 group ($p < 0.001$). No difference in p-Akt levels was observed between the control and EPI groups ($p > 0.05$).

mTOR1 levels in the EN-300 group were significantly higher than in the EPI ($p < 0.05$) and EN-50 groups. No difference in mTOR1 levels was observed between the control and NAC groups or between the control and Epi groups ($p > 0.05$).

Ki-67 levels in the EPI group were significantly higher than in the control group ($p < 0.01$) and the EN-300 group ($p < 0.01$). No difference in mTOR1 levels was observed between the control and NAC groups or between the EN-50 and EN-300 groups ($p > 0.05$).

3.3 | Analysis of Oxidative Stress and Apoptosis-Related Parameters

We measured TAS, TOS, and OSI levels in pancreatic tissue to assess oxidative stress. TAS levels in the control group were significantly higher than in the EPI group ($p < 0.01$) and significantly lower than in the NAC group ($p < 0.01$). TAS levels in the EN-50 group were significantly lower than in the EN-300 group ($p < 0.01$) and significantly higher than in the EPI group ($p < 0.01$). TOS levels were lower in the control group than in the EPI group ($p < 0.05$) and higher than in the NAC group ($p < 0.01$). TOS levels were also lower in the EN-300 group compared to the EPI group ($p < 0.01$). OSI levels were significantly higher in the EPI group than in the control ($p < 0.001$), EN-50 ($p < 0.001$), and EN-300 groups ($p < 0.001$). OSI levels were also lower in the NAC group compared to the control group ($p < 0.01$). Cleaved caspase-3 levels were significantly higher than in the control group ($p < 0.05$). Results are shown in Table 3.

TABLE 2 | Evaluation of autophagy and proliferation-related parameters between groups.

	Control	NAC	EPI	EN-50	EN-300
LC3 levels (ng/g protein)	30.40 ± 10.697	65.42 ± 28.895*	80.69 ± 53.565*	107.47 ± 47.700	46.58 ± 14.313[a]
ATG-5 levels (ng/g protein)	26.492 ± 7.131	29.798 ± 2.492	41.094 ± 3.501**	46.883 ± 8.00	28.171 ± 4.971[d]
Beclin levels (ng/mg protein)	0.396 ± 0.158	0.683 ± 0.547	0.731 ± 0.247	1.173 ± 0.249[a]	0.515 ± 0.140[d]
p-Akt levels (ng/mg protein)	0.527 ± 0.431	1.448 ± 0.501*	2.177 ± 1.790	3.60 ± 0.887	1.822 ± 0.546[c]
mTOR1 levels (ng/g protein)	56.546 ± 37.46	30.646 ± 12.55	25.642 ± 17.45	27.447 ± 11.10	64.679 ± 32.51[a,c]
Ki-67 levels (ng/mg protein)	0.695 ± 0.540	1.500 ± 1.135	2.080 ± 0.575**	1.345 ± 0.465	1.154 ± 0.194[b]

Note: Statistical analysis was performed using a one-way analysis of variance (ANOVA) followed by the Tukey post hoc test for pancreatic ATG-5 and p-AKT levels. Statistical analysis using the Kruskal–Wallis test was followed by Mann–Whitney U tests, and multiple comparisons were corrected using the Benjamini–Hochberg false discovery rate (FDR) procedure for pancreatic LC3, Beclin, and mTOR levels in pancreatic tissue. All values are presented as mean ± SD $n = 6$ per group, and $q < 0.05$ was considered significant.
Abbreviations: ATG-5, autophagy-related proteins-5; LC3, Microtubule-associated protein 1 light chain 3; mTOR, mechanistic target of rapamycin complex 1; p-AKT, phosphorylated Protein kinase B.
*$p < 0.05$ vs. control.
**p < 0.01 vs. control.
[a]$p < 0.05$ vs. EPI.
[b]$p < 0.01$ vs. EPI.
[c]$p < 0.05$ vs. EN-50.
[d]$p < 0.01$ vs. EN-50.

TABLE 3 | Evaluation of changes in oxidative stress and apoptosis related parameters between groups.

	Control	NAC	EPI	EN-50	EN-300
TAS (μmol Trolox/g protein)	0.12 ± 0.004	0.29 ± 0.311**	0.08 ± 0.034**	0.16 ± 0.011[b]	0.24 ± 0.023[b,e]
TOS (μmol H_2O_2 Eq/g protein)	2.93 ± 0.790	1.92 ± 0.562*	5.01 ± 1.53*	3.83 ± 1.24	2.25 ± 1.00[b]
OSI (arbitrary units)	22.21 ± 5.86	9.67 ± 4.30**	86.47 ± 45.3***	23.63 ± 7.13[c]	9.05 ± 3.68[c]
C-caspase-3 levels (ng/g protein)	56.68 ± 32.9	56.64 ± 25.0	99.94 ± 28.3*	87.18 ± 30.9	70.43 ± 19.3

Note: Statistical analysis was performed using a one-way analysis of variance (ANOVA) followed by the Tukey post hoc test for pancreatic TOS and OSI levels in the pancreas tissue. Statistical analysis was performed using the Kruskal–Wallis test followed by Mann–Whitney U tests, and multiple comparisons were corrected using the Benjamini–Hochberg false discovery rate (FDR) procedure for pancreatic TAS and cleaved caspase-3 levels. The OSI was calculated as follows: OSI (arbitrary units) = TOS (μmol H_2O_2 equivalent/L)/TAS (μmol Trolox equivalent/L). All values are mean ± SD $n = 6$ for each group.
Abbreviations: c-caspase-3, cleaved caspase-3; OSI, oxidative stress index; TAS, total antioxidant status; TOS, total oxidant status.
*$p < 0.05$ vs. control.
**$p < 0.01$ vs. control.
***$p < 0.001$ vs. control.
[a]$p < 0.05$ vs. EPI.
[b]$p < 0.01$ vs. EPI.
[c]$p < 0.001$ vs. EPI.
[d]$p < 0.05$ vs. EN-50.
[e]$p < 0.01$ vs. EN-50.

3.4 | Analysis of Zinc-Related Parameters

As shown in Table 4, pancreatic ZIP10 levels in the control group were significantly lower than in the NAC ($p < 0.05$) and EPI groups ($p < 0.01$). ZIP10 levels in the EN-300 group were also lower than in the EPI ($p < 0.01$) and EN-50 groups ($p < 0.05$). Pancreatic Zn levels in the control group were significantly higher than in the NAC ($p < 0.05$) and EPI groups ($p < 0.01$). NAC administration significantly reduced pancreatic Zn levels in the EN-300 group compared to the EPI group ($p < 0.05$). Plasma Zn levels in the control group were significantly lower than in the NAC group ($p < 0.05$).

3.5 | Histological Analysis

HE-stained pancreatic tissues were evaluated for edema, inflammatory cell infiltration, acinar cell degeneration, and hemorrhage (Figure 2). The histopathological scoring results for pancreatic tissues are presented in Table 5.

TABLE 4 | Evaluation of changes in zinc-related parameters between groups.

	Control	NAC	EPI	EN-50	EN-300
Pancreas ZIP-10 levels (ng/g protein)	49.035 ± 23.6	81.291 ± 21.5*	75.489 ± 29.3**	98.076 ± 31.8	56.678 ± 20.3[b,c]
Pancreas zinc levels (μg/mg protein)	6.903 ± 1.22	5.318 ± 1.04*	4.464 ± 0.843**	4.086 ± 1.86	3.305 ± 0.678**[,a]
Plasma zinc levels (μg/dL)	60.667 + 14.8	90.791 + 13.4**	73.043 + 5.01	87.345 + 21.8	64.814 + 11.7

Note: Statistical analysis was performed using the Kruskal–Wallis test, followed by Mann–Whitney U tests, and multiple comparisons were corrected using the Benjamini–Hochberg false discovery rate (FDR) procedure for pancreatic.
All values are mean ± SD $n = 6$ for each group.
*$p < 0.05$ vs. control.
**$p < 0.01$ vs. control.
[a]$p < 0.05$ vs. EPI.
[b]$p < 0.01$ vs. EPI.
[c]$p < 0.05$ vs. EN-50.

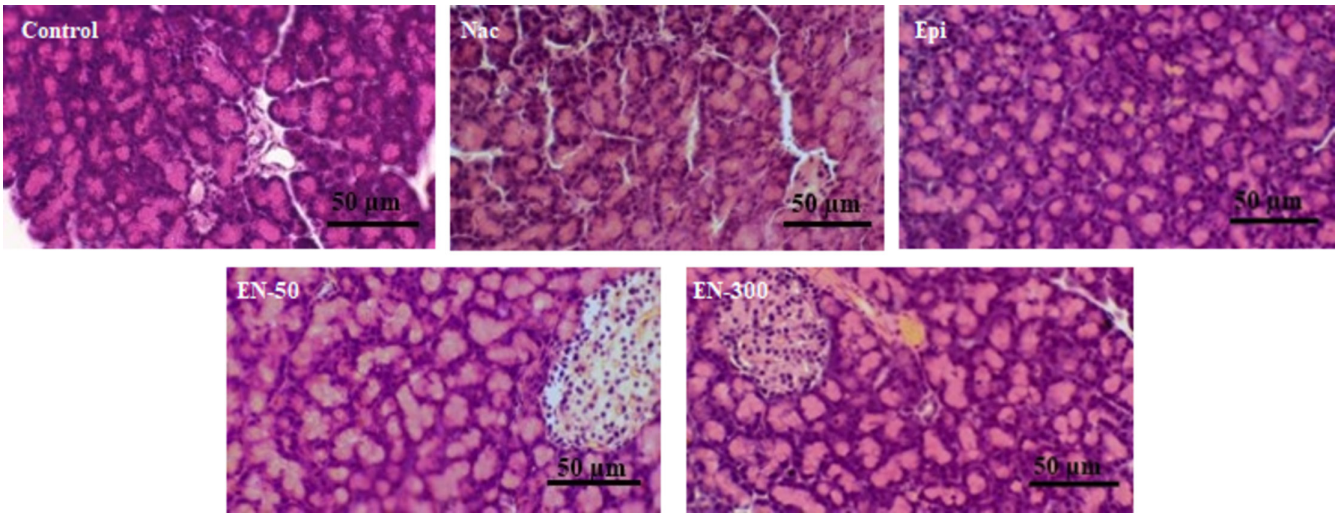

FIGURE 2 | Histological changes in the pancreas with hematoxylin and eosin stain (magnification × 40). Pancreatic sections were scored for edema, inflammatory cell infiltration, acinar cell degeneration, and hemorrhage (0 = absent/rare, 1 = mild, 2 = moderate, 3 = severe). The control and EPI groups showed normal morphology, whereas NAC induced acinar cell degeneration. EN-50 markedly reduced tissue damage compared to NAC, and EN-300 showed moderate protection.

TABLE 5 | Histopathological scores of pancreatic injury.

Parameters	Control Median (25–75)	NAC Median (25–75)	EPI Median (25–75)	EN-50 Median (25–75)	EN-300 Median (25–75)	Kruskal–Wallis H	*p*
Total score	0 (0–0)[a]	0 (0–1)	2 (2–3)[a]	1 (1–3)[a]	2 (2–3)[a,b]	146.350	< 0.001

Note: Data are presented as median (25th–75th percentile). Statistical analysis was performed using the Kruskal–Wallis test followed by the Dwass–Steel–Critchlow–Fligner post hoc test. Different superscript letters indicate statistically significant differences between groups ($p < 0.05$). $n = 6$ for each group.
[a]$p < 0.001$ vs. NAC.
[b]$p < 0.001$ vs. EN-50.

The severity of each criterion was graded on a scale of 0–3: 0: absent or rare; 1: mild; 2: moderate; 3: severe (Periyanayagam et al. 2015; Dur et al. 2016).

As shown in Table 5, pancreatic tissues in the control group exhibited normal morphology, and no significant difference was observed between the control and EPI groups ($p > 0.05$). The lowest histopathological damage scores were observed in the control and EPI groups. In the NAC group, degeneration and irregular contours were observed in the acinar cells. Histopathological damage scores in the NAC group were significantly higher than those in the control group ($p < 0.001$) and the EPI group ($p < 0.001$). Importantly, tissue damage was significantly reduced in the EN-50 group compared with the NAC group, whereas moderate damage was observed in the EN-300 group. Histopathological damage scores in the EN-50 group were significantly lower than those in the NAC group ($p < 0.001$). Similarly, the EN-300 group differed significantly from the NAC group ($p < 0.001$), although damage remained higher than in the EN-50 group. Additionally, significant differences were observed between the EPI and EN-300 groups ($p < 0.001$) and between the EN-50 and EN-300 groups ($p < 0.001$).

4 | Discussion

This study explored the impact of EPI-induced pancreatic Zn alterations on glucose homeostasis through autophagy and the modulatory role of NAC supplementation.

Zn is essential for normal pancreatic function, and both deficiency and excess are linked to diabetes (Abdulmalek and Balbaa 2019). Therefore, extracellular and intracellular Zn levels are regulated by transporter proteins, including Zn transporters (ZnTs) and importers (ZIPs, Zrt- and Irt-like proteins) (Jeong and Eide 2013). ZIP10 is a Zn importer that increases cytoplasmic Zn levels either by facilitating the uptake of extracellular Zn into the cytoplasm or by promoting the release of Zn from intracellular organelles into the cytoplasm. Additionally, studies have shown increased ZIP10 expression in pancreatic cells (Gyulkhandanyan et al. 2008; Gyulkhandanyan et al. 2006; Foster et al. 2014; Takatani-Nakase et al. 2014). Furthermore, a study demonstrated that high glucose concentrations increase ZIP10 and that intracellular Zn content in breast cancer cells (Kagara et al. 2007). In the present study, pancreatic ZIP10 levels were elevated in the Epi group compared with the control group. These findings suggest that ZIP10 may be related to Zn transport in the pancreas of the Epi group. On the other hand, our results showed reduced Zn levels in the pancreas of the Epi group, suggesting that Zn is used for insulin synthesis.

Zn is essential for insulin synthesis, storage, and secretion in β-cells. During insulin production, proinsulin is synthesized and then processed into active insulin, which is stored in secretory granules as Zn^{2+}-stabilized hexamers. Upon secretion, these hexamers dissociate into biologically active monomers, releasing Zn^{2+} ions into the extracellular space (Li 2014). In the present study, the EPI group showed significantly higher pancreatic insulin and HOMA-β levels than the control group. Moreover, plasma insulin, HOMA-IR, and plasma Zn levels were numerically higher in the EPI group than in the control group. Furthermore, no change in blood glucose levels was observed in the EPI group compared with the control group. Our results suggest a potential link between ZIP10 expression and the adaptive redistribution of Zn in β-cell processes induced by EPI. This may provide a protective response to EPI-induced cellular stress and insulin resistance, helping maintain blood glucose levels. Our findings align with previous studies linking chemotherapy agents to insulin resistance (Sharma et al. 2016). However, this interpretation should be considered hypothesis-generating rather than providing mechanistic evidence in the role of Zn and ZIP10 in this process.

Zn plays a crucial role in maintaining cell viability and regulating autophagy (Lin et al. 2020) due to its immunomodulatory, antioxidant, and anti-inflammatory properties (Jarosz et al. 2017). However, the literature is divided on the effects of Zn on autophagy. In line with this, previous research in human hepatoma cells has demonstrated that Zn deficiency suppresses autophagic activity, whereas Zn supplementation enhances it (Sun et al. 2018). Conversely, other studies show that Zn deficiency stimulates autophagy (Kawamata et al. 2017). A recent study shows that Zn depletion stimulates autophagy in yeast (Ding and Zhong 2017). Similarly, in our study, we observed decreased pancreatic Zn levels and elevated levels of LC3, Beclin1, and ATG5, indicating enhanced autophagy (Pasquier 2016) in the EPI group compared to the control group. Our findings suggest that autophagy may be increased in the pancreas as a defense against EPI-induced stress.

Supporting this view, excessive production of ROS during oxidative stress can stimulate autophagy as a protective mechanism against cellular injury and apoptosis (Zhu et al. 2022). Consistent with earlier findings (Alves et al. 2016), the present study found that EPI treatment increased TOS and OSI levels, enhanced apoptotic activity, decreased TAS levels, increased Ki-67 levels, and preserved morphological structure in the Epi group. Recent studies have shown that ROS play a key role in triggering autophagy in response to chemotherapy-induced stress (Silva and Peixoto 2018; Choi et al. 2017). Chittaranjan et al. also reported that Ki-67 production was increased in the EPI-resistant cells (Chittaranjan et al. 2014). In this respect, our results are consistent with studies showing that autophagy is an adaptive response to oxidative stress (Rossin et al. 2025) and promotes cell survival and proliferation (Niranjan et al. 2021; Wang et al. 2020). Furthermore, our results suggest that this adaptive response may help preserve the Epi group's morphological structure against oxidative stress.

In the EN-50 and EN-300 groups, NAC administration reduced OSI levels in pancreatic tissue compared with the Epi group. These findings align with studies showing beneficial effects at both doses (Sabbaghziarani et al. 2024; Kalimeris et al. 2016). Furthermore, the more pronounced reduction in oxidative stress with high-dose NAC compared with low-dose NAC suggested that high-dose NAC is more effective at lowering oxidative stress. Additionally, high-dose NAC administration reduced LC3 and Ki-67 levels in the EN-300 group compared with the Epi group, suggesting that high-dose NAC is more effective at inhibiting autophagy and proliferation. Zn levels in the EN-300 group were also reduced, and this reduction was greater than in the EPI group. Interestingly, although autophagy was suppressed in the EN-300, it was not suppressed in the EPI group. These findings suggest that varying degrees of Zn deficiency

may differentially regulate autophagy-related cellular signaling pathways. Because small changes in signaling molecules may lead to substantial alterations in signaling pathway dynamics and cellular responses (Afsar and Kantar 2025).

Autophagy is tightly regulated by the AMP-activated protein kinase (AMPK) and the Akt/mTORC1 signaling pathways. Under energy stress, AMPK activation promotes autophagy by inhibiting mTORC1 (Pasquier 2016). Zn deficiency disrupts mitochondrial function and energy metabolism, lowering the ATP/AMP ratio and activating AMPK (Kim et al. 2022; Kong et al. 2020). Similarly, Kim et al. demonstrated that Zn deficiency in neuronal cells affects the AMPK/mTOR pathway, thereby increasing autophagy (Kim et al. 2022). However, severe ATP depletion may impair autophagic flux by disrupting ATP-dependent lysosomal acidification and other energy-requiring autophagic processes (Mandic et al. 2024). Moreover, Zn deficiency has been shown to impair mitochondrial respiratory function and ATP production, thereby contributing to metabolic stress and altered autophagic signaling (Sun et al. 2016; Liu et al. 2021). In our study, mTOR1 levels were decreased in the EPI group but increased in the EN-300 group relative to the EPI group. Therefore, our findings suggest that mild Zn deficiency may trigger adaptive survival responses, whereas more severe Zn deficiency may disrupt cellular homeostasis and suppress autophagy under severe metabolic stress. In addition, autophagy regulation may have occurred through modulation of mTOR1 signaling. However, the role of mTOR1 in autophagy inhibition may be mediated by the AMPK pathway rather than the AKT/mTOR pathway, because p-AKT levels did not increase despite elevated mTOR1 in the EN-300 group.

Our findings are consistent with previous studies demonstrating the bidirectional effects of Zn deficiency on autophagy (Ding and Zhong 2017; Sun et al. 2018). Moreover, reduced Zn levels may be due to lower ZIP10 levels in the EN-300 group. Supporting this view, a study demonstrated that ZIP10 upregulation serves as an adaptive mechanism to maintain intracellular Zn availability (Shim et al. 2025). However, further studies are needed to develop a precise mechanistic understanding of how autophagy is regulated in the EPI group, particularly the roles of Zn, ZIP10, and AMPK-related signaling in modulating autophagy. In the NAC-only group, TAS levels increased, whereas TOS and OSI levels decreased relative to the control group. However, mild degeneration and contour irregularities were observed in pancreatic acinar cells. Although suppression of oxidative stress is generally protective, excessive reduction of ROS levels may impair physiological redox signaling, disrupt cellular homeostasis, and contribute to reductive stress-related cellular dysfunction (Schieber and Chandel 2014). Therefore, the morphological alterations observed in pancreatic tissue of the NAC group may be associated with excessive suppression of ROS generation and disruption of normal redox signaling. NAC is a versatile agent widely used in clinical and experimental settings; however, its limitations and potential toxic effects remain incompletely elucidated (Tsai et al. 2024; Ershad et al. 2026). Our findings are consistent with a study showing that excessive NAC administration causes hepatic toxicity by disrupting GSH and reducing ATP levels (Tsai et al. 2024). Our findings also highlight the differential effects of NAC dosage on pancreatic function in EPI-treated rats. Insulin levels in the pancreas were higher in the EN-50 group than in the EPI group; however, they were similar to those of the EPI group in the EN-300 group. This pattern may be related to the effects of high doses of NAC on the pancreas, as morphological improvement was observed in the EN-50 group compared to the NAC group, but this improvement was more limited in the EN-300 group. In this respect, our findings are consistent with studies showing that high doses of NAC may be associated with organ toxicity.

In the early stages of type 2 diabetes, compensatory hyperinsulinemia develops in response to insulin resistance, whereas progressive β-cell dysfunction in later stages results in impaired insulin secretion and relative hypoinsulinemia (Lu et al. 2024). Supporting this, a population-based study of 1168 non-diabetic adolescents and adults found that individuals with the highest insulin secretion levels had greater adiposity, less favorable lipid profiles, and reduced glucose tolerance (Trico et al. 2018). The 2016 case report also described an individual with breast cancer treated with EPI who developed symptoms suggestive of DM after chemotherapy (Sharma et al. 2016). Taken together, these findings suggest that the molecular alterations observed in pancreatic tissue of the EPI group may reflect a profile predictive of diabetes risk. NAC treatment can worsen these diabetic conditions.

As a result, NAC administration exerted beneficial effects against EPI-mediated oxidative stress, but it may also adversely affect pancreatic morphology. These findings indicate that NAC may have therapeutic potential for reducing EPI-induced oxidative stress–related side effects; however, its effects should be interpreted cautiously, and further mechanistic and experimental studies are needed to clarify its safety and biological impact on pancreatic tissue.

5 | Conclusion

In summary, our study suggests that EPI-induced changes in pancreatic Zn levels may trigger compensatory mechanisms, including autophagy, to maintain insulin secretion and mitigate oxidative stress-induced damage. NAC supplementation had dose-dependent effects on these processes: low-dose NAC (EN-50) reduced oxidative stress and enhanced insulin synthesis, whereas high-dose NAC (EN-300) appeared to reduce autophagy and impair pancreatic function. Furthermore, Zn may regulate autophagy via mTOR1 in a dose-dependent manner; accordingly, decreased Zn in the Epi group may have increased autophagy, whereas more severe Zn deficiency in the EN-300 group may have suppressed autophagy. Collectively, these findings highlight the intricate interplay among Zn homeostasis, autophagy, and oxidative stress in pancreatic function and underscore the importance of antioxidant dosage in modulating adaptive cellular responses under chemotherapeutic stress.

6 | Limitations

This study has several limitations. First, pharmacokinetic data (including plasma drug concentrations) in rats were not analyzed to confirm the dose equivalence of the selected EPI dose.

Second, pancreatic-specific toxicity assessment was not conducted in the NAC-only group.

Third, the hypothesis that excessive antioxidant activity could lead to reductive stress was not directly tested.

Fourth, the absence of a positive autophagy control group limits mechanistic interpretation.

Fifth, investigation of Zn and ZIP10 localization, functional zinc transport assays, or other zinc transporters could help explain the observed findings.

Author Contributions

E.A. designed the study, performed biochemical and statistical analyses, and interpreted the results. I.E. performed hematoxylin and eosin staining analyses and evaluated these results.

Acknowledgments

The authors have nothing to report.

Funding

The authors have nothing to report.

Ethics Statement

Ethics approval was provided by the Institutional Animal Care and Use Committee at Aksaray University (2025/4-37).

Consent

The authors have nothing to report.

Conflicts of Interest

The authors declare no conflicts of interest.

Data Availability Statement

The data supporting this study's findings are available from the corresponding author, upon reasonable request.

References

Abdulmalek, S. A., and M. Balbaa. 2019. "Synergistic Effect of Nano-Selenium and Metformin on Type 2 Diabetic Rat Model: Diabetic Complications Alleviation Through Insulin Sensitivity, Oxidative Mediators and Inflammatory Markers." *PLoS ONE* 14, no. 8: e0220779. https://doi.org/10.1371/journal.pone.0220779.

Afsar, E., K. Dogan, E. Arslan, et al. 2026. "Does Zn-Mediated Regulation of the Kynurenine Pathway Provide the Link Between Periodontal Disease and Diabetes?" *Biological Trace Element Research* 204, no. 1: 1–12. https://doi.org/10.1007/s12011-025-04776-x.

Afsar, E., and D. Kantar. 2025. "How Does Zinc Chelation Affect Liver Sphingolipid Metabolism in an Alzheimer's-Like Model?" *Journal of Trace Elements in Medicine and Biology* 87. https://doi.org/10.1016/j.jtemb.2025.127589.

Afsar, E., M. Öz, and I. Eranil. 2026. "Hepato-Cardiac Axis in Epirubicin Toxicity: Role of Kynurenine Pathway and N-Acetylcysteine Antioxidant Intervention." *Journal of Applied Toxicology*. https://doi.org/10.1002/jat.70118.

Alves, A. C., D. Ribeiro, C. Nunes, and S. Reis. 2016. "Biophysics in Cancer: The Relevance of Drug-Membrane Interaction Studies." *Biochimica et Biophysica Acta* 1858, no. 9: 2231–2244. https://doi.org/10.1016/j.bbamem.2016.06.025.

Bradford, M. M. 1976. "A Rapid and Sensitive Method for the Quantitation of Microgram Quantities of Protein Utilizing the Principle of Protein-Dye Binding." *Analytical Biochemistry* 72: 248–254. https://doi.org/10.1016/0003-2697(76)90527-3.

Chittaranjan, S., S. Bortnik, W. H. Dragowska, et al. 2014. "Autophagy Inhibition Augments the Anticancer Effects of Epirubicin Treatment in Anthracycline-Sensitive and -Resistant Triple-Negative Breast Cancer." *Clinical Cancer Research* 20, no. 12: 3159–3173. https://doi.org/10.1158/1078-0432.CCR-13-2060.

Choi, J. H., S. W. Jin, C. Y. Choi, et al. 2017. "Capsaicin Inhibits Dimethylnitrosamine-Induced Hepatic Fibrosis by Inhibiting the Tgf-Beta1/Smad Pathway via Peroxisome Proliferator-Activated Receptor Gamma Activation." *Journal of Agricultural and Food Chemistry* 65, no. 2: 317–326. https://doi.org/10.1021/acs.jafc.6b04805.

Devaleriola, D. 1994. "Dose Optimization of Anthracyclines." *Anticancer Research* 14, no. 6a: 2307–2313 <go to ISI>://WOS:A1994QE79200008.

Ding, B., and Q. Zhong. 2017. "Zinc Deficiency: An Unexpected Trigger for Autophagy." *Journal of Biological Chemistry* 292, no. 20: 8531–8532. https://doi.org/10.1074/jbc.H116.762948.

Dobbs, N. A., C. J. Twelves, W. Gregory, C. Cruickshanka, M. A. Richards, and R. D. Rubens. 2003. "Epirubicin in Patients with Liver Dysfunction: Development and Evaluation of a Novel Dose Modification Scheme." *European Journal of Cancer* 39, no. 5: 580–586. https://doi.org/10.1016/s0959-8049(02)00669-x.

Dobbs, N. A., C. J. Twelves, P. Rizzi, et al. 1994. "Epirubicin in Hepatocellular Carcinoma: Pharmacokinetics and Clinical Activity." *Cancer Chemotherapy and Pharmacology* 34, no. 5: 405–410. https://doi.org/10.1007/BF00685565.

Dur, A., H. Kose, A. Kocyigit, O. Kocaman, M. Ismayilova, and F. C. Sonmez. 2016. "The Anti-Inflammatory and Antioxidant Effects of Thymoquinone on Ceruleine Induced Acute Pancreatitis in Rats." *Bratislavské Lekárske Listy* 117, no. 10: 614–618. https://doi.org/10.4149/bll_2016_119.

Ershad, M., A. Naji, P. Patel, and D. Vearrier. 2026. *N-Acetylcysteine*. Statpearls. https://www.ncbi.nlm.nih.gov/pubmed/30725868.

Ersoz, E., M. S. Aydin, Y. Hacanli, et al. 2023. "Cardioprotective Effect of *Pistacia vera* L. (Green Pistachio) Hull Extract in Wistar Albino Rats With Doxorubicin-Induced Cardiac Damage." *Anatolian Journal of Cardiology* 27, no. 3: 135–145. https://doi.org/10.14744/AnatolJCardiol.2022.2452.

Foster, M., A. Chu, P. Petocz, and S. Samman. 2014. "Zinc Transporter Gene Expression and Glycemic Control in Post-Menopausal Women With Type 2 Diabetes Mellitus." *Journal of Trace Elements in Medicine and Biology* 28, no. 4: 448–452. https://doi.org/10.1016/j.jtemb.2014.07.012.

Gyulkhandanyan, A. V., S. C. Lee, G. Bikopoulos, F. Dai, and M. B. Wheeler. 2006. "The Zn^{2+}–Transporting Pathways in Pancreatic Beta-Cells: A Role for the L-Type Voltage-Gated Ca^{2+} Channel." *Journal of Biological Chemistry* 281, no. 14: 9361–9372. https://doi.org/10.1074/jbc.M508542200.

Gyulkhandanyan, A. V., H. Lu, S. C. Lee, et al. 2008. "Investigation of Transport Mechanisms and Regulation of Intracellular Zn^{2+} in Pancreatic Alpha-Cells." *Journal of Biological Chemistry* 283, no. 15: 10184–10197. https://doi.org/10.1074/jbc.M707005200.

Jarosz, M., M. Olbert, G. Wyszogrodzka, K. Mlyniec, and T. Librowski. 2017. "Antioxidant and Anti-Inflammatory Effects of Zinc. Zinc-Dependent Nf-Kappab Signaling." *Inflammopharmacology* 25, no. 1: 11–24. https://doi.org/10.1007/s10787-017-0309-4.

Jeong, J., and D. J. Eide. 2013. "The Slc39 Family of Zinc Transporters." *Molecular Aspects of Medicine* 34, no. 2–3: 612–619. https://doi.org/10.1016/j.mam.2012.05.011.

Kagara, N., N. Tanaka, S. Noguchi, and T. Hirano. 2007. "Zinc and Its Transporter Zip10 Are Involved in Invasive Behavior of Breast Cancer Cells." *Cancer Science* 98, no. 5: 692–697. https://doi.org/10.1111/j.1349-7006.2007.00446.x.

Kalimeris, K., P. Briassoulis, A. Ntzouvani, et al. 2016. "N-Acetylcysteine Ameliorates Liver Injury in a Rat Model of Intestinal Ischemia Reperfusion." *Journal of Surgical Research* 206, no. 2: 263–272. https://doi.org/10.1016/j.jss.2016.08.049.

Kawamata, T., T. Horie, M. Matsunami, M. Sasaki, and Y. Ohsumi. 2017. "Zinc Starvation Induces Autophagy in Yeast." *Journal of Biological Chemistry* 292, no. 20: 8520–8530. https://doi.org/10.1074/jbc.M116.762948.

Kim, S. Y., J. H. Lee, and S. A. Kim. 2022. "Zinc Deficiency Induces Autophagy in Ht-22 Mouse Hippocampal Neuronal Cell Line." *International Journal of Molecular Sciences* 23, no. 15: 8811. https://doi.org/10.3390/ijms23158811.

Kong, D. S., Z. L. Zhang, L. P. Chen, et al. 2020. "Curcumin Blunts Epithelial-Mesenchymal Transition of Hepatocytes to Alleviate Hepatic Fibrosis Through Regulating Oxidative Stress and Autophagy." *Redox Biology* 36. https://doi.org/10.1016/j.redox.2020.101600.

Kong, F. J., J. H. Wu, S. Y. Sun, and J. Q. Zhou. 2017. "The Endoplasmic Reticulum Stress/Autophagy Pathway Is Involved in Cholesterol-Induced Pancreatic B-Cell Injury." *Scientific Reports* 7: ARTN 44746. https://doi.org/10.1038/srep44746.

Lee, S., and D. K. Lee. 2020. "What Is the Proper Way to Apply the Multiple Comparison Test? (Vol 71, Pg 353, 2018)." *Korean Journal of Anesthesiology* 73, no. 6: 572–572. https://doi.org/10.4097/kja.d.18.00242.e1.

Li, H. Y., X. Shen, M. J. Ma, et al. 2021. "Zip10 Drives Osteosarcoma Proliferation and Chemoresistance Through Itga10-Mediated Activation of the Pi3k/Akt Pathway." *Journal of Experimental & Clinical Cancer Research* 40, no. 1: 340. https://doi.org/10.1186/s13046-021-02146-8.

Li, Y. V. 2014. "Zinc and Insulin in Pancreatic Beta-Cells." *Endocrine* 45, no. 2: 178–189. https://doi.org/10.1007/s12020-013-0032-x.

Lin, S., H. Tian, J. Q. Lin, et al. 2020. "Zinc Promotes Autophagy and Inhibits Apoptosis Through Ampk/Mtor Signaling Pathway After Spinal Cord Injury." *Neuroscience Letters* 736: ARTN 135263. https://doi.org/10.1016/j.neulet.2020.135263.

Liu, H. Y., J. R. Gale, I. J. Reynolds, J. H. Weiss, and E. Aizenman. 2021. "The Multifaceted Roles of Zinc in Neuronal Mitochondrial Dysfunction." *Biomedicine* 9, no. 5: 489. https://doi.org/10.3390/biomedicines9050489.

Liuzzi, J. P., and R. Pazos. 2020. "Interplay Between Autophagy and Zinc." *Journal of Trace Elements in Medicine and Biology* 62: ARTN 126636. https://doi.org/10.1016/j.jtemb.2020.126636.

Lu, X., Q. X. Xie, X. H. Pan, et al. 2024. "Type 2 Diabetes Mellitus in Adults: Pathogenesis, Prevention and Therapy." *Signal Transduction and Targeted Therapy* 9, no. 1: ARTN 262. https://doi.org/10.1038/s41392-024-01951-9.

Mandic, M., V. Paunovic, L. Vucicevic, et al. 2024. "No Energy, No Autophagy-Mechanisms and Therapeutic Implications of Autophagic Response Energy Requirements." *Journal of Cellular Physiology* 239, no. 11. https://doi.org/10.1002/jcp.31366.

Nair, A. B., and S. Jacob. 2016. "A Simple Practice Guide for Dose Conversion Between Animals and Human." *Journal of Basic and Clinical Pharmacy* 7, no. 2: 27–31. https://doi.org/10.4103/0976-0105.177703.

Niranjan, R., K. P. Mishra, S. N. Tripathi, and A. K. Thakur. 2021. "Proliferation of Lung Epithelial Cells Is Regulated by the Mechanisms of Autophagy Upon Exposure of Soots." *Frontiers in Cell and Developmental Biology* 9. https://doi.org/10.3389/fcell.2021.662597.

Ozturk, E., O. Balat, Y. G. Acilmis, C. Ozcan, S. Pence, and Ö. Erel. 2011. "Measurement of the Placental Total Antioxidant Status in Preeclamptic Women Using a Novel Automated Method." *Journal of Obstetrics and Gynaecology Research* 37, no. 4: 337–342. https://doi.org/10.1111/j.1447-0756.2010.01346.x.

Pasquier, B. 2016. "Autophagy Inhibitors." *Cellular and Molecular Life Sciences* 73, no. 5: 985–1001. https://doi.org/10.1007/s00018-015-2104-y.

Periyanayagam, S., G. Arumugam, A. Ravikumar, and V. S. Ganesan. 2015. "Thymoquinone Ameliorates Nlrp3-Mediated Inflammation in the Pancreas of Albino Wistar Rats Fed Ethanol and High-Fat Diet." *Journal of Basic and Clinical Physiology and Pharmacology* 26, no. 6: 623–632. https://doi.org/10.1515/jbcpp-2014-0109.

Petit, K., M. Suwalsky, J. R. Colina, et al. 2020. "Toxic Effects of the Anticancer Drug Epirubicin in Vitro Assayed in Human Erythrocytes." *Toxicology in Vitro* 68: 104964. https://doi.org/10.1016/j.tiv.2020.104964.

Rossin, D., M. G. Perrelli, M. Lo Iacono, R. Rastaldo, and C. Giachino. 2025. "Dynamic Interplay Between Autophagy and Oxidative Stress in Stem Cells: Implications for Regenerative Medicine." *Antioxidants* 14, no. 6: 691. https://doi.org/10.3390/antiox14060691.

Sabbaghziarani, F., P. Soleimani, F. R. Eynshikh, F. Zafari, and E. Aali. 2024. "Reduced Ischemia-Reperfusion Oxidative Stress Injury by Melatonin and N-Acetylcysteine in the Male Rat Brain." *IBRO Neuroscience Reports* 17: 131–137. https://doi.org/10.1016/j.ibneur.2024.07.004.

Schieber, M., and N. S. Chandel. 2014. "Ros Function in Redox Signaling and Oxidative Stress." *Current Biology* 24, no. 10: R453–R462. https://doi.org/10.1016/j.cub.2014.03.034.

Sharma, P. K., A. K. Misra, V. Singh, A. Gupta, S. Saroha, and S. Singh. 2016. "Cyclophosphamide and Epirubicin-Induced Diabetes Mellitus in Breast Cancer: A Rare Occurrence." *Journal of Pharmacology and Pharmacotherapeutics* 7, no. 3: 146–148. https://doi.org/10.4103/0976-500X.189684.

Sheng, Q., X. Xiao, K. Prasadan, et al. 2017. "Autophagy Protects Pancreatic Beta Cell Mass and Function in the Setting of a High-Fat and High-Glucose Diet." *Scientific Reports* 7, no. 1: 16348. https://doi.org/10.1038/s41598-017-16485-0.

Shim, G., M. J. Kim, and M. S. Ryu. 2025. "Zinc Transporter Zip10 Supports Zinc Homeostasis and Myoglobin Biosynthesis in Differentiating C2c12 Myoblasts." *Frontiers in Cell and Developmental Biology* 13: ARTN 1691317. https://doi.org/10.3389/fcell.2025.1691317.

Shojaee Barjoee, S., V. Rodionov, and R. N. Neda. 2025. "Occupational Injuries Associated With Safety Climate Among Ceramic Industry Workers in Iran." *Scientific Reports* 15: 24585. https://doi.org/10.1038/s41598-025-09704-6.

Silva, A. K. S., and C. A. Peixoto. 2018. "Role of Peroxisome Proliferator-Activated Receptors in Non-Alcoholic Fatty Liver Disease Inflammation." *Cellular and Molecular Life Sciences* 75, no. 16: 2951–2961. https://doi.org/10.1007/s00018-018-2838-4.

Sun, Q., W. Zhong, W. L. Zhang, and Z. X. Zhou. 2016. "Defect of Mitochondrial Respiratory Chain Is a Mechanism of Ros Overproduction in a Rat Model of Alcoholic Liver Disease: Role of Zinc Deficiency." *American Journal of Physiology-Gastrointestinal and Liver Physiology* 310, no. 3: G205–G214. https://doi.org/10.1152/ajpgi.00270.2015.

Sun, W., J. Yang, W. Wang, et al. 2018. "The Beneficial Effects of Zn on Akt-Mediated Insulin and Cell Survival Signaling Pathways in Diabetes." *Journal of Trace Elements in Medicine and Biology* 46: 117–127. https://doi.org/10.1016/j.jtemb.2017.12.005.

Takatani-Nakase, T., C. Matsui, S. Maeda, S. Kawahara, and K. Takahashi. 2014. "High Glucose Level Promotes Migration Behavior of Breast Cancer Cells Through Zinc and its Transporters." *PLoS ONE* 9, no. 2: e90136. https://doi.org/10.1371/journal.pone.0090136.

Trico, D., A. Natali, S. Arslanian, A. Mari, and E. Ferrannini. 2018. "Identification, Pathophysiology, and Clinical Implications of Primary Insulin Hypersecretion in Nondiabetic Adults and Adolescents." *JCI Insight* 3, no. 24. https://doi.org/10.1172/jci.insight.124912.

Tsai, M. S., G. G. Liou, J. W. Liao, et al. 2024. "N-Acetyl Cysteine Overdose Induced Acute Toxicity and Hepatic Microvesicular Steatosis by Disrupting Gsh and Interfering Lipid Metabolisms in Normal Mice." *Antioxidants* 13, no. 7. https://doi.org/10.3390/antiox13070832.

Tuohetaerbaike, B., Y. Zhang, Y. Tian, et al. 2020. "Pancreas Protective Effects of Urolithin a on Type 2 Diabetic Mice Induced by High Fat and Streptozotocin via Regulating Autophagy and Akt/Mtor Signaling Pathway." *Journal of Ethnopharmacology* 250: 112479. https://doi.org/10.1016/j.jep.2019.112479.

Wang, J. Y., N. Kaplan, S. J. Wang, et al. 2020. "Autophagy Plays a Positive Role in Induction of Epidermal Proliferation." *FASEB Journal* 34, no. 8: 10657–10667. https://doi.org/10.1096/fj.202000770RR.

Zhu, C. Y., S. W. Shen, S. H. Zhang, M. Huang, L. Zhang, and X. Chen. 2022. "Autophagy in Bone Remodeling: A Regulator of Oxidative Stress." *Frontiers in Endocrinology* 13: 898634. https://doi.org/10.3389/fendo.2022.898634.